

# Three - Way- Catalyst- Monolith Converters (Pt- Loaded) for Gasoline Engine: Experimental Study and Modeling

Intisar Hussain Aljumily<sup>1</sup>, Farah Talib Al-Sudani<sup>2</sup>, Zaidoon Muhsen<sup>3</sup>  
University of Technology, Chemical Engineering Department, Baghdad, Iraq.

1 Email: [intisar59@yahoo.com](mailto:intisar59@yahoo.com), 2 Email: [falsudany@yahoo.com](mailto:falsudany@yahoo.com), 3 Email: [dr\\_zaidoon@yahoo.com](mailto:dr_zaidoon@yahoo.com)

## ABSTRACT

In this study the experimental and theoretical investigation have been carried out to study the performance of Commercial

ceramic monolith catalyst with Pt loading of 0.5, 1, and 1.5 wt% on the oxidation and reduction of exhaust gas (NO, CO, and HC) emitted from gasoline generator. The results showed that the increase in metal content leads to the decreasing of performance of the commercial ceramic monolith catalyst. Also the Pt loading over commercial ceramic monolith catalyst improves the CO oxidation rather than HC oxidation and NO reduction. One-dimensional heterogeneous (reactor and pellet) and axial dispersion model of non-isothermal operation was applied to describe a single channel of the monolith. This model takes into account both intra and surface concentration and temperature gradients within channel. Concentration profile along the reactor and into intra-catalyst dimension for the reactants and products were estimated.

## INTRODUCTION

The reduction of CO, NO and hydrocarbon emissions from automotive exhaust gases has been extensively studied in the past two decades (Granger et al., 2002). The catalytic monolith reactor has been widely used as a pollution abatement device for reducing the emission of CO, NO and hydrocarbon, because of its structural integrity and unique advantages such as high heat and mass transfer rates per unit pressure drop, high specific interfacial area, and ease of scale-up compared to packed-bed or ceramic foam reactors. It consists of a matrix of a large number of parallel channels of about 1mm hydraulic diameter. The catalysts deposited in the form of a wash coat (of typical average thickness of 10 - 250 nm) on the inner walls of the channel. As the reacting fluid flows along the channel, the reactants diffuse transverse to the flow direction from the bulk gas phase in to the washcoat where they diffuse and react on the active catalyst sites (Wang et al., 2011). The oxidation of CO and hydrocarbons and reduction of NO<sub>x</sub> takes place simultaneously in the complex porous structure of catalytic washcoat layer which are formed by  $\gamma$ -Al<sub>2</sub>O<sub>3</sub> support

(alumina) with dispersed crystallites of noble metals (typically Pt) as catalytic sites (Koci et al., 2004). The selective reduction of nitrogen oxide by various hydrocarbons was investigated with alumina and silica supported Pt catalyst by Burch et al., 1997. They found the tendency to produce N<sub>2</sub>O in substantial quantities (typically up to 65% of the NO is converted in to N<sub>2</sub>O). Fabiano et al., 2007, found that the methane conversion and CO selectivity increased with used of higher Pt content. Wang et al., 2011 added the Pt to beta zeolite-Al<sub>2</sub>O<sub>3</sub>/cordierite, the Pt/beta zeolite-Al<sub>2</sub>O<sub>3</sub>/cordierite monolith exhibited good performance for the catalytic purification of automobile exhaust from real lean-burn engine. The main pollutants NO<sub>x</sub>, HC and CO can be simultaneously purified at 300–400 °C. In the present work, the performance of Pt/Al<sub>2</sub>O<sub>3</sub> with Pt loading of 0.5, 1, and 1.5 wt% on the treatment of exhaust gas emission from gasoline generator has been investigated experimentally and theoretically.

## EXPERIMENTAL Work CHARACTERISTIC OF THE SUPPORT

Monolithic catalyst was made of ceramic honeycomb substrate. The chemical composition was  $\gamma$ -Al<sub>2</sub>O<sub>3</sub> 69.76%, SiO<sub>2</sub> 11.3%, Fe<sub>2</sub>O<sub>3</sub> 9.4%, CeO<sub>2</sub> 6.75%, BaO 2.6%, TiO<sub>2</sub> 0.01%, CuO 0.02%, Rh 0.16%. The main physical parameters of honeycomb support are presented in Table 1.

**Table 1. physical properties of commercial monolith catalyst.**

| Physicals Properties                          |        |
|---|--------|
| Channel Structure                             | Circle |
| Number of channels, channel / cm <sup>2</sup> | 64     |
| Channel spacing, mm                           | 1.4    |
| Wall thickness, mm                            | 0.3    |
| Wall porosity %                               | 60     |
| Bulk density, g / cm <sup>3</sup>             | 1.4    |
| Pore volume, cm <sup>3</sup> / gm             | 0.93   |
| Surface area, m <sup>2</sup> / g              | 97     |

### Coating of the Commercial Monolithic Catalyst

Commercial catalysts containing from 0.5 to 1.5wt% Pt were prepared by an incipient wetness impregnation method from an aqueous solution of hexachloroplatinic acid ( $H_2(PtCl_6) \cdot 6 H_2O$ ) as described elsewhere (Richardson 1989). The loaded monolith with 0.5 wt% Pt was prepared by suspending 14.02 gm of commercial monolith catalyst. The amount of platinum needed for loading monolith was calculated from the weight of catalyst sample and the amount of metal in impregnation solution are presented in Table 2. The same procedures were carried out to determine the amount of reagents used for preparation of 1, 1.5 %wt Pt. Table 3 shows the properties of the prepared catalysts. The physical properties were determined by Petroleum Research and Development Center and Production and Metallurgy Department of University of Technology.

**Table 2: The amount of reagents used for preparation of 0.5, 1, 1.5 %wt pt catalysts**

| No. | wt. of catalyst sample, gm | Pt Wt% | wt. of metal gm | wt. of salt gm |
|-----|----------------------------|--------|-----------------|----------------|
| 1   | 14.1                       | 1.5    | 0.2115          | 0.5616         |
| 2   | 14.05                      | 1      | 0.1405          | 0.373          |
| 3   | 14.02                      | 0.5    | 0.07            | 0.184          |

**Table 3 : The properties of the prepared catalysts**

| Catalyst Specification     | 0.5%Pt | 1%Pt | 1.5%Pt |
|----------------------------|--------|------|--------|
| Surface area, $m^2/g$      | 85     | 61   | 48     |
| bulk density, $g/cm^3$     | 1.48   | 1.5  | 1.53   |
| Porosity                   | 0.44   | 0.38 | 0.31   |
| Equivalent pore radius, nm | 8      | 7.1  | 6.6    |

### Experimental Apparatus and Procedures

The reactor system consisted of tubular reactor (I.D 2 cm, length 20 cm), electrical heater, thermocouple, flow meter and gas analysis equipment. The monolith catalyst with length 10cm was placed into the reactor. Before the reaction, the monolithic catalyst had been reduced at 750K for 5 hours under 1000GHSV of hydrogen and cooled to the desired reaction temperature. The exhaust gas emission from the gasoline generator was treated under atmospheric pressure at 200-500°C, various GSV ( $8.8-35.5 s^{-1}$ ) and Pt loading (0.5, 1, 1.5%). Temperature of reactant gas was monitored by thermocouple (Ni-CrNi) placed at the exit of the monolith. Space times were changed by varying flow rate of the reactant gas over constant volume of the catalyst monolith. The reaction products were analyzed by gas chromatography (shimadzu-14A), thermal conductivity detector with helium as carrier gas. Fig.1 shows the experimental setup.

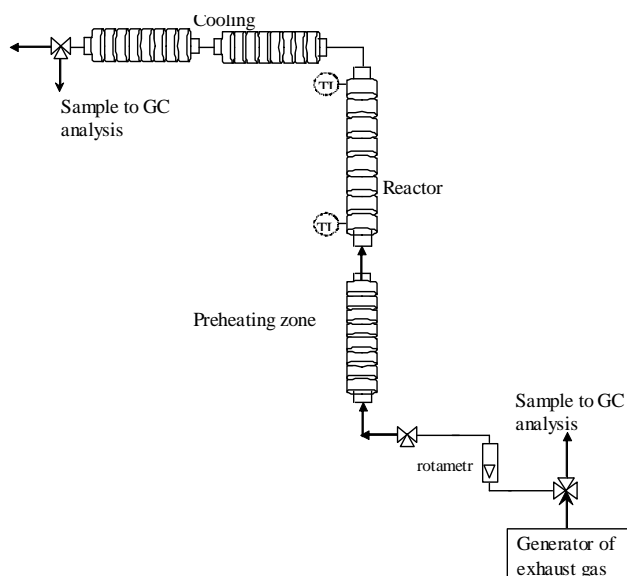


**Fig.1. Experimental Setup**

### Mathematical model.

#### Assumption and model equations

A spatially 1D axial dispersion heterogeneous model was used to simulate a single channel of the monolith reactor which generally depends on:

- Description of the reactant flow along the channels
- Kinetic model of a chemical reaction
- Heat and mass transfer in fluid and solid phases

The following assumptions regarded as acceptable and convenient for the present work were made:-

- Steady state and non-isothermal conditions.
- Fully developed laminar flow inside the channel.
- Negligible pressure drop along the monolith channel
- Non-ideal plug flow (1D dispersion model).
- Circle geometry of the channel after wash coating (due to a thin layer of the wash coat).
- No change in fluid physical properties due to reaction.
- All the transport properties are well distributed cross-sectionally and vary only with axial location

According to the above assumptions, the model is represented by the following equation:-

**Reactor Model**

$$\epsilon^g D_{a,k} \frac{\partial^2 C_k}{\partial y^2} - \epsilon^g u \frac{\partial C_k}{\partial y} + k_{ca} (C_k - C_{k,s}) = 0 \dots \dots \dots (1)$$

$$k_{ca} (C_k - C_{k,s}) - [\rho_p (\sum u_k \cdot r_k)] * (1 - \epsilon^g) \vartheta_s = 0 \dots (2)$$

**Pellet Model**

$$D_{e,k} \frac{\partial^2 C_{k,s}}{\partial x^2} = R_k \dots \dots \dots (3)$$

Where  $R_k = \rho_p \cdot r_k (1 - \epsilon^g) \vartheta_s$

**Enthalpy Balance**

$$\epsilon^g k_{a,k} \frac{\partial^2 T_f}{\partial y^2} - \epsilon^g \rho_c u \frac{\partial T_f}{\partial y} + h_k a (T_f - T_s) = 0 \dots \dots \dots (4)$$

$$\delta_w k_w \frac{\partial^2 T_s}{\partial y^2} + h_k a (T_f - T_s) + \vartheta_s \sum (-\Delta H_{r,k}) R_k = 0 \dots (5)$$

**Boundary Conditions**

- The boundary conditions for reactor model at the inlet (y=0) of the monolith reactor are :-

$$C_k^G \Big|_{y=0} = \frac{P_k}{RT}$$

- The boundary conditions after passing the entrance

$$D_{a,k} \frac{\partial C_k^G}{\partial y} = u_g (C_k^{G,o+} - C_k^G \Big|_{y=0})$$

- Inside the catalyst pore the boundary conditions

are:-  $\frac{\partial C_k^S}{\partial x} \Big|_{x=0} = -\frac{k_k}{D_{ei}} (C_k^G - m C_k^S)$

$$\frac{\partial C_k^S}{\partial x} \Big|_{x=L_c} = 0$$

- For energy balance , the boundary conditions over the entire reactor length  $T_s = T_1$
- The boundary conditions

At reactor inlet  $T_f \Big|_{y=0} = T_G \Big|_{y=0} = T_o, \frac{\partial T_f}{\partial y} = 0$

$$\frac{\partial T_f}{\partial y} = \frac{\partial T_s}{\partial y} = 0$$

At y=L (end of the reactor)

**Numerical Solution**

The model equations were solved using MATLAB 7.0 running under WINDOWS 7. One-dimensional channel model was used to predict the performance of monolith reactor. This model takes into account both intra and

surface concentration and temperature gradients within channel and washcoat layer. The mole and energy balances within the reactor and washcoat comprise a system of non-linear partial differential equations were solved simultaneously taken into account the initial and boundary conditions within the system. Finite Element Method (FEM) was used to solve the model equations by converting the partial differential equations into a system of algebraic equations corresponding to a finite number of predetermined mesh points, the algebraic equations was solved later by Gaussian elimination method.

A FEM was also used to calculate the effectiveness factors, both external and internal mass transfer resistance were taken into account.

The equations were solved iteratively, in which each of the six profiles (five for gas concentrations and one for temperature) were solved iteratively until overall convergence was achieved. The mass-transfer coefficients for gas phase was where calculated using the Equations cited in West et al,2003. Table 4 shows the range of the effectiveness factors of the present work.

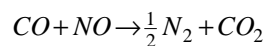
**Table 4 : The range of the effectiveness factors of the present work.**

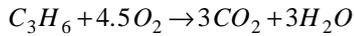
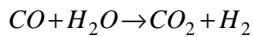
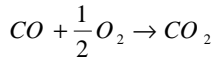
| Reaction                                     | Range of effectiveness factor |
|--|-------------------------------|
| $CO + NO \rightarrow \frac{1}{2} N_2 + CO_2$ | $0.9316 \leq \eta \leq 0.98$  |
| $CO + \frac{1}{2} O_2 \rightarrow CO_2$      | $0.5521 \leq \eta \leq 0.64$  |
| $CO + H_2O \rightarrow CO_2 + H_2$           | $0.9985 \leq \eta \leq 0.99$  |
| $C_3H_6 + 4.5 O_2 \rightarrow 3CO_2 + 3H_2O$ | $0.9049 \leq \eta \leq 0.98$  |

**ESTIMATION REACTION KINETIC PARAMERTERS**

**Kinetic modeling**

Heterogeneous reaction of exhaust gas was used to model the monolith catalytic performance and symbolically written as follows:-





The kinetic reaction rate is considered to follow simple power law kinetics expression, in general form (Fogler

Scott, 1997) :- where  $k_i = A \exp\left(\frac{-E_a}{RT}\right)$

The reaction rate constant  $k_i$  confirms the Arrhenius

expression:-  $\ln k_i = \ln A - \frac{E_a}{RT}$

The kinetic expression is to be non-linear (m, n th order with respect both reactants) under the present reaction.

$$r_i = k_i C_A^m C_B^n$$

### Kinetic modeling

The kinetic experiments were modeled iteratively by comparing conversions and temperature generated from the mathematical model with the experimental conversions and temperature using least square approximation method. A set of 16 experiments for each catalyst loading was modeled to determine the rate parameters for the model. The kinetic coefficients in the reactions were optimized by Nelder-Mead optimization method.

The apparent activation energy, pre-exponential factor and reaction orders for each reaction within the system were directly optimized within the optimization procedure by adjusting the model to the experimental. The estimation of the  $k_0$ ,  $n$  and  $m$  was performed by minimizing the objective function through **fmincon** command. The objective function, that is the minimum squares sum, was utilized as an adjust criterion in an optimization routine for the estimation of the parameters and also for the comparison of the simulated model with the experimental data. The determined optimized parameters for kinetic rates and activation energies are presented in Table 5.

**Table 5** : Apparent activation energy values and reaction order for commercial catalyst and different loading metal.

| Reaction   | E <sub>a</sub> KJ / mol | A <sub>0</sub> | Reaction order |       |
|--|-------------------------|----------------|----------------|-------|
|  |                         |                | N              | m     |
| 1.5% Pt  |                         |                |                |       |
| NO + CO  | 29.569                  | 38.074         | 0.2104         | 0.854 |
| CO + ½ O <sub>2</sub>                              | 22.018                  | 20.0001        | 0.2891         | 0.730 |
| CO + H <sub>2</sub> O                              | 40.023                  | 0.1548         | 0.2299         | 1.927 |
| C <sub>3</sub> H <sub>6</sub> + 4.5 O <sub>2</sub> | 26.542                  | 18.964         | 0.9844         | 0.737 |
| 1% Pt  |                         |                |                |       |
| NO + CO  | 22.1312                 | 47.571         | 1.2174         | 1.229 |
| CO + ½ O <sub>2</sub>                              | 18.149                  | 26.782         | 2.0000         | 0.1   |
| CO + H <sub>2</sub> O                              | 33.424                  | 0.288          | 2.0000         | 0.1   |
| C <sub>3</sub> H <sub>6</sub> + 4.5 O <sub>2</sub> | 20.953                  | 20.766         | 2.0000         | 0.1   |
| 0.5% Pt  |                         |                |                |       |
| NO + CO  | 15.428                  | 62.706         | 1.9314         | 1.311 |
| CO + ½ O <sub>2</sub>                              | 11.7                    | 37.061         | 2              | 0.3   |
| CO + H <sub>2</sub> O                              | 30.493                  | 0.3            | 2              | 0.3   |
| C <sub>3</sub> H <sub>6</sub> + 4.5 O <sub>2</sub> | 18.428                  | 38.860         | 2              | 0.639 |

## THERMO-PHYSICAL AND REACTOR PROPERTIES.

### PHYSICAL PROPERTIES

The physical properties for the gas used in the present work viscosity, density, heat capacity, thermal conductivity, heat of formation, effective diffusivity and Knudsen diffusivity were estimated from standard correlations reported by Reid, et al, 1977 and Perry et al, 1997, Kolaczowski and Hays, 1997.

### EXTERNAL HEAT AND MASS TRANSFER COEFFICIENT

The heat and mass transfer coefficients along the monolith channel ( $k_c(y)$  and  $h(y)$ ) used here in the present model were calculated from the proper correlations cited in West et al, 2003.

## RESULTS AND DISCUSSION

### EXPERIMENTAL WORK

#### Effect of Operating Conditions

- **Effect of Temperature**

The influence of temperature in the range of (200-500 °C) on the exhaust gas conversion and rate of reaction as a function of gas space velocity at a given type of loading catalyst (0.5%Pt), is shown in Fig. (2 - 4). It can be seen from these figures that the conversion of exhaust gas increases with increasing temperature. This is attributed to the increasing of diffusivity of

molecular gases. The activation energies for the oxidation of CO and HC at a given temperature are lower than the reduction of NO as shown in Table 4 . The same behavior was obtained for the other Pt% loading as shown in Fig. 4 .These results are in agreement with the results obtained by Granger et al, 2002 and Hoebink et al., 2002.

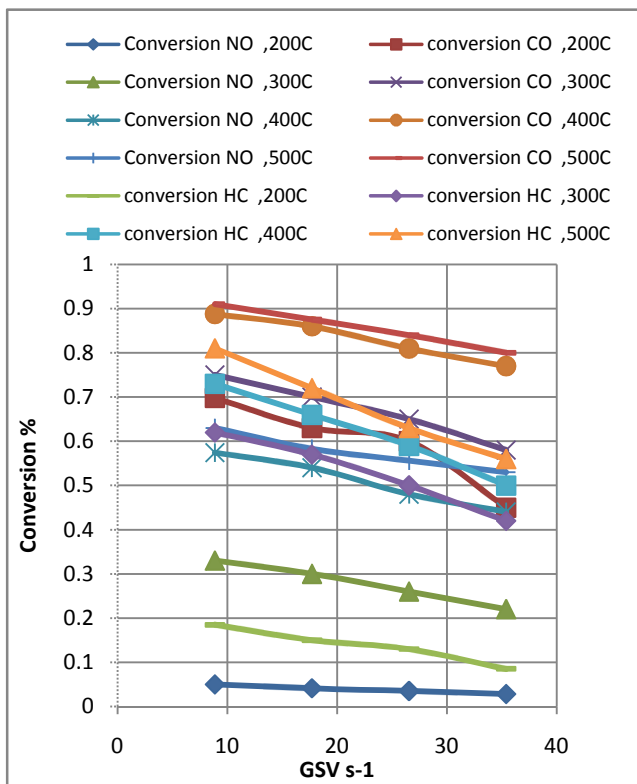


Fig. 2. Effect of reaction temperature on conversion at 1.5% Pt as a function of GSV

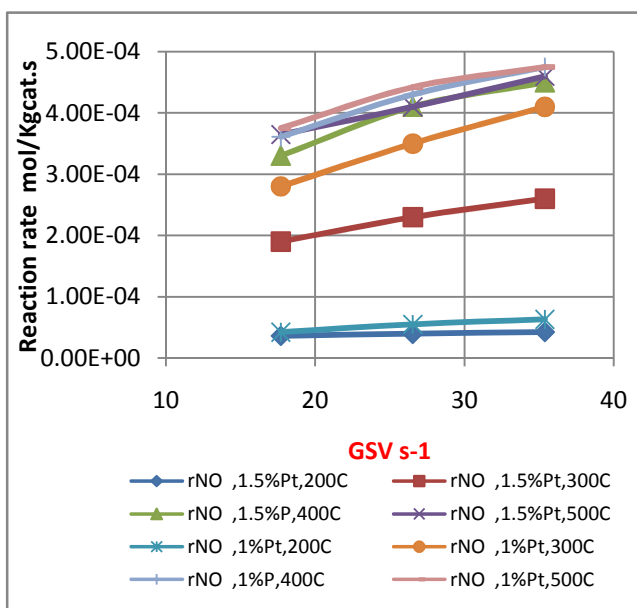


Fig. 3. Effect of reaction temperature on rate reaction as a function of % Pt loaded and GSV

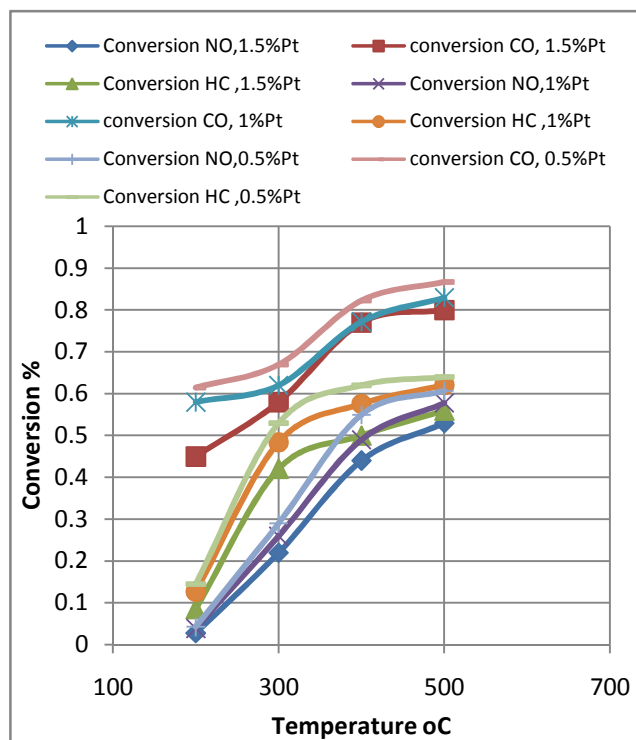


Fig. 4. Effect of reaction temperature on conversion at GSV 35.4s<sup>-1</sup> and as a function of Pt% loading

#### • Effect of GSV

The effect of gas space velocity in the range of (8.8-35.4 s<sup>-1</sup>) on the conversion and reaction rate of exhaust gas at a given Pt loading (1.5%) for commercial monolith catalyst and for different types of loading catalyst can be seen in Fig. 2-3, and 5 . It can be noticed from these figures that the conversion of the exhaust gas decreases while reaction rates increase with increasing gas velocity, owing to decrease in the residence time (decreasing contact time of the feed reactant) with the catalyst inside reactor, such trends are in agreement with the observation of previous finding of Williamsson et al., 1989 , Tomasic et al., 1998 and Fabiano et al., 2007.

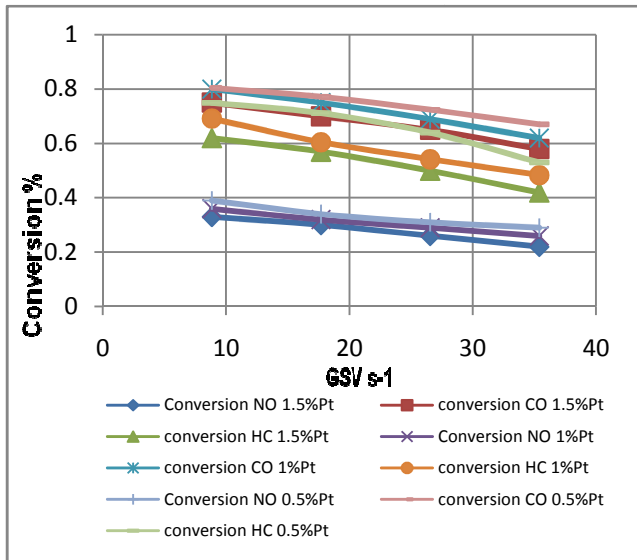


Fig. 5. Effect of GSV on conversion at 200 °C and as a function of Pt% loading

• Effect of Pt Loading

Fig. 3-5 show the effect 0.5 , 1 and 1.5% wt Pt on the conversion and reaction rate of exhaust gases. From these figures ,it can be seen that the conversion of NO reduction and CO and HC oxidation using 0.5% loading catalyst is higher than those obtained by 1%Pt and 1.5% Pt . This may be attributed to the lower apparent activation energy of the NO reduction and CO ,HC oxidation over 0.5% Pt loading catalyst compared with the 1 and 1.5% Pt ( see Table 4). Also the surface area of 0.5%Pt is higher than those of 1 and 1.5%Pt lead to the improvement of the metallic dispersion on the surface of the support which enhances the reaction rate. These results agree with those obtained by Gonzales-Velasco et al., 1999, Granger et al., 2002 and Fabiano et al ,2007.

It seems from Fig.4 that 0.5%Pt gives the lower light off temperature (50% conversion) compared with other Pt loaded catalyst, this is attributed to that 0.5%Pt reach higher conversion at lower temperature . Similar results were obtained by Paloma et al., 2004. .Also Fig. 4 shows that Pt loading over commercial ceramic monolith catalyst improve the CO oxidation rather than HC oxidation and NO reduction.

**SIMULATION RESULTS AND DISCUSSION**

The proposed model in the present work is tested for the CO , HC oxidation and NO reduction system.

Fig. 6 and 7 show the concentration profile of exhaust gases along the reactor and catalyst surface respectively. It can be seen that NO,CO, and HC concentration decreases along the reactor length.

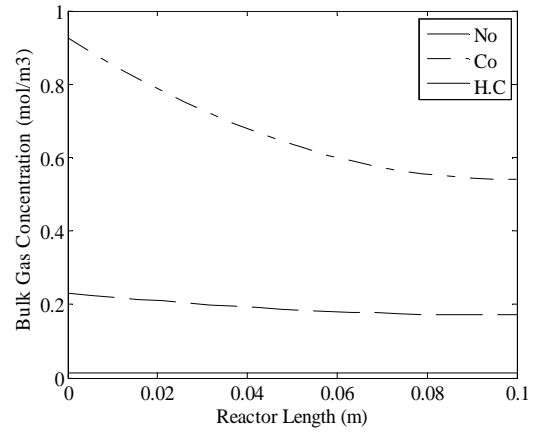


Fig. 6. Model result for CO, NO an HC concentrations in bulk along the reactor (0.5 % Pt , T=200 C, Ug=1.769 m/s)

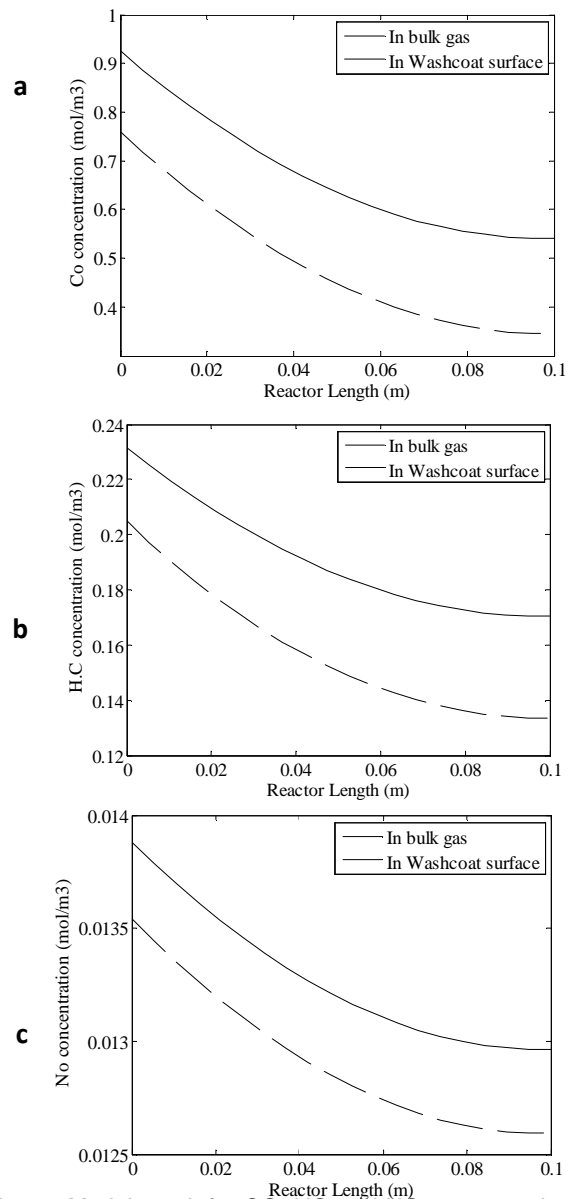


Fig. 7. Model result for CO, NO and HC concentrations in bulk along the reactor and catalyst surface (0.5 % Pt , T=200 C, Ug=1.769 m/s)

From Fig.7 it can be seen that CO concentration decreases significantly along the reactor as compared with NO and HC. This emphasizes that the Pt loading over the commercial monolith catalysts improves the CO oxidation rather than HC oxidation and NO reduction.

From Fig. 8 it can be noticed that the concentration gradient of NO, CO, and HC through the catalyst depth is slightly decreased. This indicates that internal diffusion limitations can be neglected. This is attributed to higher activation energy larger than 10Kcal/mol which emphasizes that rate is kinetically controlled (Farruto and Bartholomew ,1997 and Morbidelli et al.,2001).

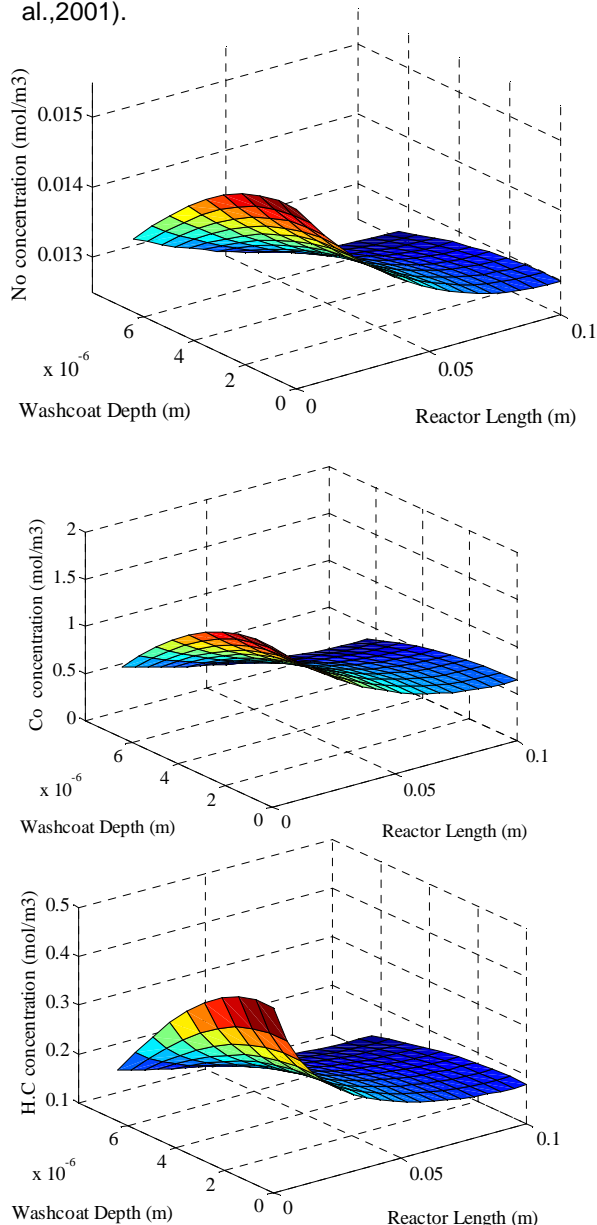


Fig . 8. Model results for NO ,CO , and H.C concentration profile in along reactor and washcoat depth (0.5 % PT , T=200 C, Ug=1.769 m/s)

Fig.9. gives the trend of temperature profile which increases along the reactor. From this figure, it can be seen that the surface temperature is higher than the bulk temperature due to the reaction being exothermic.

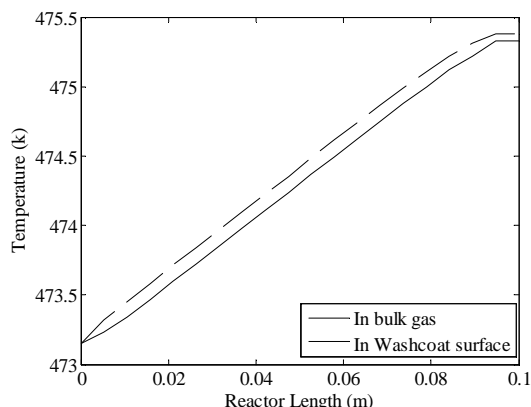


Fig.9. Model result for Temperate profile in bulk and washcoat surface along the reactor (0.5 % PT , T=200 C, Ug=1.769 m/s)

The simulation results as shown in Fig.10 can capture the broad trends of the experimental observed data.

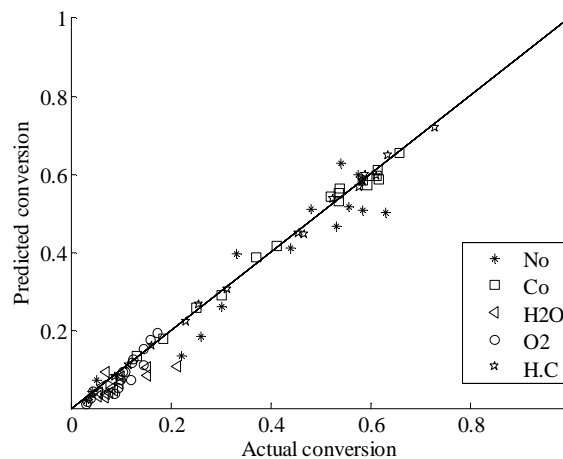


Fig. 10. Comparison between actual and model predicted conversions for 16 experiments (0.5 % Pt , T=200 C, Ug=1.769 m/s)

## CONCLUSIONS

The main points concluded from the present study are summarized as follows:-

- The increase of metal content leads to decreasing of performance of the commercial ceramic monolith catalyst.
- Pt loading over commercial ceramic monolith catalyst improves the CO oxidation rather than HC oxidation and NO reduction.
- The conversion of exhaust gas increases with increasing temperature, activation energies for

the oxidation of CO and HC are lower than the reduction of NO.

- The conversion of the exhaust gas decreases while reaction rates increases with increasing gas velocity.

## Nomenclatures

|            |   |  |
|------------|---|--|
| A          | Pre-exponential factor of reaction-kinetic constant | ( - )  |
| A          | Interfacial area                                    | $m^2/m^3$                                      |
| C          | Concentration                                       | $mol/m^3$                                      |
| $C_p$      | Molar heat capacity of gas                          | $J/mol.K$                                      |
| $D_a$      | Axial dispersion coefficient                        | $m^2/s$  |
| $D_e$      | Effective diffusivity                               | $m^2/s$  |
| $E_a$      | Activation energy                                   | $kJ/mol$                                       |
| h          | Heat transfer coefficient                           | $J/m^2 . s K$                                  |
| $\Delta H$ | Heat of reaction                                    | $kJ/mol$                                       |
| $K_a$      | Fluid thermal conductivity                          | $w/m^2.k$                                      |
| $K_c$      | Mass transfer coefficient                           | $m/s$  |
| $K_i$      | Reaction rate constant                              | $\frac{mol^{1-(n+m)}}{kg_{cat} .s m^{3(n+m)}}$ |
| $k_w$      | Thermal conductivity of washcoat                    | $w/m^2.k$                                      |
| L          | Length of reactor                                   | M  |
| $L_C$      | Characteristic length                               | m  |
| M          | Henrys constant                                     | $kg/kg mol$                                    |
| P          | Pressure  | atm  |
| R          | Gas constant  | $m^3.atm /mol K$                               |
| $R_i$      | Reaction rate of species i component                | $mol/m^3_{cat}.s$                              |
| r          | Reaction rate                                       | $mol/kg_{cat}.s$                               |
| $T_b$      | Temperature   | K  |
| T          | Time  | S  |
| U          | Superficial velocity                                | $m/s$  |
| x          | Length inside pore coordinates                      | M  |
| Y          | Axial coordinate                                    | m  |

## Subscripts & Superscripts

|       |                             |
|-------|-----------------------------|
| A,B   | Component A and B           |
| B     | Bulk value                  |
| f     | Fluid                       |
| k     | Series species of component |
| m     | Reaction order              |
| n     | Reaction order              |
| o     | Inlet condition             |
| $o^+$ | After entrance              |
| s     | Solid surface value         |
| p     | Particle                    |
| G     | Gas phase                   |
| 1     | Set point                   |

## Greek Symbols

|              |                                      |          |
|--------------|--------------------------------------|----------|
| $\nu^s$      | Fraction of wash coat in solid phase | ( - )    |
| $\epsilon^g$ | Void fraction of reactor             | ( - )    |
| $\eta$       | Effectiveness factor                 | ( - )    |
| $\rho$       | Density                              | $kg/m^3$ |

## REFERENCES

- Burch R. and D. Ottery .1997. The selective reduction of nitrogen oxide by higher hydrocarbons on Pt catalyst under lean-burn conditions. *Applied Catalyst B: Environmental* 13: 105-111.
- Fabiano S., S.Diego da, A.Juan, and Fabio B. 2007. The effect of Pt/CeZrO<sub>2</sub>/Al<sub>2</sub>O<sub>3</sub> catalysts for the partial oxidation of methane. *Studies in surface science and catalysis* 167: 427-432.
- Farrauto R. and C.Bartholomew .1997. Fundamentals of industrial catalytic process, Kluwer Scientific Publishers, Amsterdam.
- Fogler Scott, H. 1997.Element of chemical reaction engineering . Prentice-Hall of India Private Limited.
- Gonzales-Velasco J., M.Jeam, and B.Gilbert. 1999 . Contribution of Cerium/Zirconium mixed oxides to the activity of a new generation of TWC. *Applied Catalyst B: Environmental* 22: 167-178.
- Granger P., J.LeComete, and G.Leclercq. 2002. Kinetics of the CO+NO reaction over bimetallic platinum-rhodium on alumina, Effect of ceria in corporation into noble metals. *Journal of Catalyst* 207: 202-212.
- Hoebink J., R.Van Gemert, and G. Marin .2002. Modeling of the NOx conversion maximum in the light-off curves under net oxidizing condition. *Chemical Engineering Science* 55: 1573-1581.
- Mladenov , N., J. Koop, S. Tischer, and O. Deutschmann .2010. Modeling of transport and chemistry in channel flows of automotive catalytic converters. *Chemical Engineering Science*, 65: 812-826.
- Morbideilli, M. ,A. Garvriilidis ,and A. Varma .2001. catalyst design: Optimal distribution of catalyst in pellets ,Reactors and membranes .Cambridge Univ.Press.Cambridge Uk.
- Koci,P. , M. Kubicek and M. Marek. 2004 . Multifunctional aspects of three – way catalyst effects of complex washcoat composition. *Chem.Eng.Res &Des* 82:284-292.

Kolaczkowski S.T. , R.E, Hayes ,and . 1997. Introduction to catalytic composition .Gordon and Breach Science publisher.

Reid R., J. Prausnitz, and B. Poling .1987. The properties of gases and liquids. New-York: Hemisphere-McGraw-Hill.

Perry, R.H., and W.G. Don. 1997Perry's chemical engineers' handbook . New York: McGraw-Hill.

Richardson J. 1989 . Principles of catalyst development, plenum press . New York :Hemisphere-McGraw-Hill.

Paloma H., O.Salvador, and D.Fernand .2004. Composition of methane over palladium catalyst in the presence of inorganic compounds. Applied Catalyst B: Environmental 47:85-93.

Tomasic V., Z. Gomzi, and S. Zrncvic .1998. Catalytic reduction of NOx over Cu/25M.5 catalyst. Applied Catalyst B: Environmental 18:233-240.

Wang, T., S. Yang, and K. Sun, X. Fang.2011. Preparation of Pt/beta zeolite–Al<sub>2</sub>O<sub>3</sub>/cordierite. Ceramics International : 37 , 621–626

West, D.H. , V. Balakotaiah and Z. Jovanoic .2003 . Experimental and theoretical investigation of the mass transfer controlled regime in catalytic monoliths. Catal.Today 88:8-14.

Williamson W., M. Summers, and J. Skowron .1989. Catalyst technology for future automotive emission system. SAE 88:103-110